CHIN. PHYS. LETT. Vol. 38, No. 4 (2021) 045202

Nonlinear Simulations of the Bump-on-Tail Instabilities in Tokamak Plasmas

Yumei Hou(侯玉梅)*, Wei Chen(陈伟)*, Liming Yu(于利明), Yunpeng Zou(邹云鹏), Min Xu(许敏), and Xuru Duan(段旭如)

Southwestern Institute of Physics, Chengdu 610041, China

(Received 30 November 2020; accepted 25 January 2021; published online 6 April 2021)

We reproduce nonlinear behaviors, including frequency chirping and mode splitting, referred to as bump-on-tail instabilities. As has been reported in previous works, the generation and motion of phase-space hole-clump pairs in a kinetically driven, dissipative system can result in frequency chirping. We provide examples of frequency chirping, both with and without pure diffusion, in order to illustrate the role of the diffusion effect, which can suppress holes and clumps; Asymmetric frequency chirpings are produced with drag effect, which is essential to enhance holes, and suppress clumps. Although both diffusion and drag effect suppress the clumps, downward sweepings are observed, caused by a complicated interaction of diffusion and drag. In addition, we examine the discrepancies in frequency chirping between marginally unstable, and far from marginally unstable cases, which we elucidate by means of a dissipative system. In addition, mode splitting is also produced via BOT code for a marginal case with large diffusion.

DOI: 10.1088/0256-307X/38/4/045202

Alfvén waves driven by energetic particles have been observed in many magnetic confinement fusion devices,[1–3] and are regarded as desirable channels for energy transport via strong wave-particle resonance.[4] Moreover, they provide valuable information regarding core burning plasma conditions. However, they may also redistribute and eject energetic particles, causing damage to the first wall, and significant deterioration in terms of plasma confinement.[5–7]

It is generally understood that nonlinear physics deals with nonlinear wave-particle interactions and nonlinear wave-wave interactions.[8–9] In order to better understand these nonlinear physical processes, a number of experimental and simulation studies have been performed. Alfvén waves with rapid and periodic frequency sweeping, a phenomenon known as chirping, have been observed in numerous fusion devices, such as DIII-D,[10] JT-60U,[11] MAST,[12] NSTX,[13] and HL-2A.[14] Various types of numerical simulation code, such as BOT,[15–18] δf-COBBLES,[19] MEGA,[20]GTC,[21] XHMGC,[22] and EAC[23] have been employed to illustrate these nonlinear dynamics. Alfvén waves exhibiting frequency splitting have been studied both theoretically and experimentally.[24–25] In addition, the Berk–Breizman model[26–28] has been applied in order to interpret both frequency chirping and frequency splitting.

The Berk–Breizman model is a reduced one-dimensional weakly nonlinear theory, used to describe the nonlinear behaviors observed in fusion devices. The bump-on-tail distribution function is characterized by a distinctive bump in the high velocity region, where an electrostatic wave is destabilized by energetic particles. Let us suppose an electrostatic wave, with a frequency ω, and a wave number k; the gradient of the distribution function is positive at $v = \omega/k$ (refer to Fig. 9 in Ref. [16]), leading to the growth of the wave via resonant interaction. The Berk–Breizman model describes the nonlinear evolution of a bump-on-tail distribution function with a Maxwellian bulk, a weak beam, and a small electrostatic perturbation. Here, the background dissipative mechanisms are assumed to be external wave damping and a collision operator. A representative equation for the bump-on-tail problem, established by Berk, and extended by Lilley, was introduced in Ref. [15]:

$$\begin{aligned}\frac{dA}{d\tau} = A(\tau) - \frac{1}{2}\int_0^{\tau/2} dz z^2 A(\tau - z) \cdot \int_0^{\tau-2z} dx \\ \cdot \exp[-\hat{\nu}_{\rm d}^3 z^2\Big(\frac{2z}{3} + x\Big) - \hat{\nu}_\alpha(2z + x) \\ + i\hat{\nu}_{\rm f}^2 z(z + x)] \cdot A(\tau - z - x)A^*(\tau - 2z - x),\end{aligned} \tag{1}$$

where $\tau = (\gamma_{\rm L} - \gamma_{\rm d})t$, $\hat{\nu}_{\rm d}^3 = \nu_{\rm d}^3/(\gamma_{\rm L} - \gamma_{\rm d})^3$, $\hat{\nu}_\alpha = \nu_\alpha/(\gamma_{\rm L} - \gamma_{\rm d})$, and $\hat{\nu}_{\rm f}^2 = \nu_{\rm f}^2/(\gamma_{\rm L} - \gamma_{\rm d})^2$; $\gamma_{\rm L}$ is the kinetic drive in the absence of dissipation, and $\gamma_{\rm d}$ is the intrinsic damping rate from the bulk plasmas. Here, $\nu_{\rm d}$, $\nu_{\rm f}$ and ν_α represent velocity-space diffusion, dynamical drag (Fokker–Plank collision includes diffusion and drag), and Krook collision, respectively. Both

Supported by the National Key R&D Program of China (Grant No. 2019YFE03020000), the National Natural Science Foundation of China (Grant Nos. 11875021, 11875024, and 12005054), and the Sichuan Science and Technology Program (Grant No. 2020JQQN0070).

*Corresponding authors. Email: houym@swip.ac.cn; chenw@swip.ac.cn

© 2021 Chinese Physical Society and IOP Publishing Ltd

$\nu_{\rm d}$ and $\nu_{\rm f}$ include contributions from the pitch-angle scattering term and parallel velocity diffusion, and $\nu_{\rm f}$ also includes a contribution from the slowing-down term. Numerical solutions to Eq. (1) illustrate that four typical regimes are exhibited: steady-state, periodic, chaotic, and explosive. These can be reproduced using BOT code. The chaotic regime significantly accounts for the frequency chirping observed in the experiments. In addition, with the help of BOT code, nonlinear behaviors, such as hooked frequency chirping and undulating regimes, are observed, in the presence of both drag and diffusion.[12]

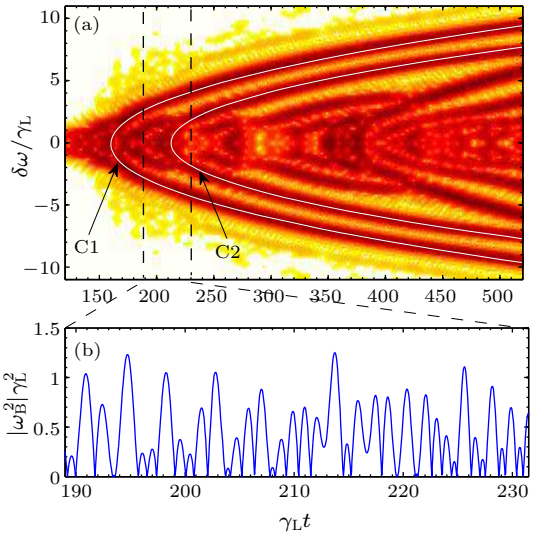

Fig. 1. (a) Spectrogram of continuous frequency chirping, where $\gamma_{\rm d}/\gamma_{\rm L} = 0.9$, and $\hat{\nu}_{\rm d} = \hat{\nu}_{\rm f} = \hat{\nu}_{\alpha} = 0$. The first and second branches are labeled C1 and C2 (white solid line), respectively. (b) Zoomed-in area showing the time evolution of the bounce frequency during $\gamma_{\rm L}t = 190$–230.

A nonlinear scenario close to the instability threshold ($|\gamma_{\rm L} - \gamma_{\rm d}| \ll \gamma_{\rm d} \leq \gamma_{\rm L}$), and in the absence of collisions ($\nu_{\rm d} = \nu_{\rm f} = \nu_{\alpha} = 0$), is produced using BOT code. A Fourier spectrogram of ideal continuous frequency chirping is illustrated in Fig. 1(a). The wave frequency symmetrically shifts up and down from the original eigenfrequency. The first and second branches are labeled C1 and C2, respectively. These results differ slightly from the experimental data (see Fig. 1 in Ref. [14]), as the frequency shifts continuously, without a break point. The time evolution of the bounce frequency during $\gamma_{\rm L}t = 190$–230 is presented in Fig. 1(b) as $\omega_{\rm B} = (ek\hat{E}/m)^{\frac{1}{2}}$, where $\hat{E}\cos(\omega t - kx)$ is the perturbing longitudinal electric field. Given that the lines shown in Fig. 1(b) are irregular, according to Fig. 2 in Ref. [26], the continuous frequency chirping belongs to a chaotic regime.

It is understood that if the phase space plateau is excited in the wave-particle's resonance region, then holes (a depletion of particles) and clumps (an excess of particles) in the perturbed particle distribution function arise, and detach from one another [see Fig. 2(a)]. The motion is synchronized to the change in wave frequency, which shifts up and down from the original eigenfrequency [Fig. 1(a)], facilitating energy transportation, whereby power is nonlinearly extracted from the resonant energetic particles, or dissipated into the background plasma. When $\gamma_{\rm L}t = 190$, the original hole-clump pairs are generated, characterized by a group of eye-shaped areas, which are associated with the first set of strong chirping components (C1) in Fig. 1(a) [Fig. 2(a)]. The first set of hole-clump pairs then detach, while secondary pairs (C2) are formed in the original resonance plane when $\gamma_{\rm L}t = 230$ [Fig. 2(b)]. As the particle number is conserved in the system, the motion of hole-clump pairs will steepen the gradient of the distribution function (see Fig. 9 in Ref. [16]), making the system unstable once again, so that subsequent pairs then occur in rapid succession, giving rise to continuous frequency chirping.

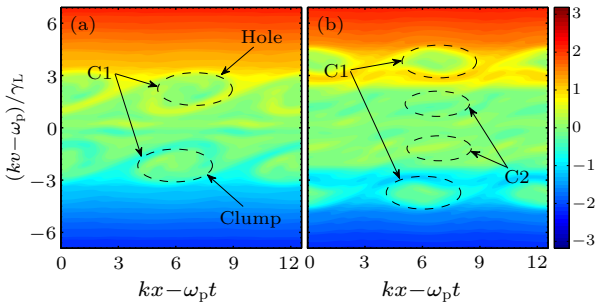

Fig. 2. Phase space portraits for fast particle distribution, corresponding to Fig. 1(a) (black dashed lines). (a) The original hole-clump pairs (C1) are generated, exhibiting a group of eye-shaped areas when $\gamma_{\rm L}t = 190$. (b) The first set of hole-clump pairs (C1) detach, while the second pairs (C2) are formed in the resonance plane when $\gamma_{\rm L}t = 230$.

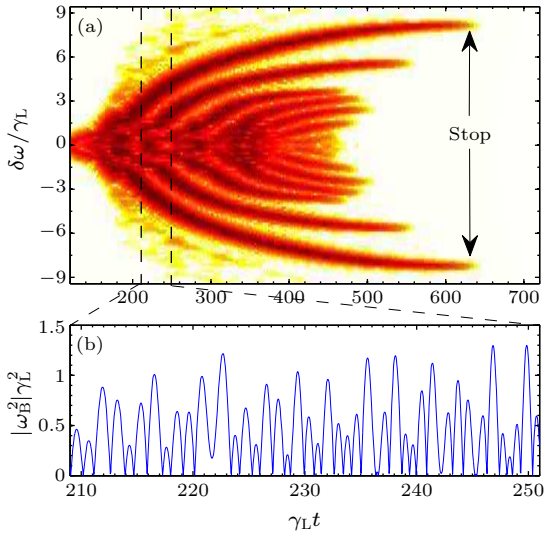

Fig. 3. (a) Spectrogram of symmetric frequency chirping, where $\gamma_{\rm d}/\gamma_{\rm L} = 0.9$, and $\hat{\nu}_{\rm d} = 0.88$, $\hat{\nu}_{\rm f} = \hat{\nu}_{\alpha} = 0$. (b) Zoomed-in area depicting the time evolution of the bounce frequency during $\gamma_{\rm L}t = 210$–250.

Next, we investigate frequency chirping in a marginally unstable case with pure diffusion. A Fourier spectrogram, together with the time evolution of the bounce frequency, are presented in Fig. 3. The process of generation, detachment, and erosion of hole-clump pairs is indicative of competition between the field of the mode and the diffusion effect. In other words, the wave-particle interactions produce the perturbed plateau and generate hole-clump pairs which flatten the perturbed particle distribution function near the resonance (see Fig. 4 in Ref. [17]), which is interrupted by the diffusion effect, which fills the hole and depletes the clump, resulting in an obvious break [Fig. 3(a)]. The time evolution of the bounce frequency during $\gamma_{\rm L}t = 210$–250 reveals that this type of frequency chirping also belongs to a chaotic regime.

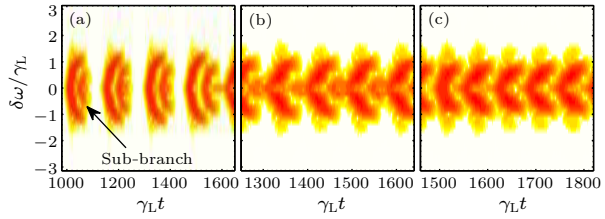

Fig. 4. Spectrogram of symmetric frequency chirping far from marginal stability, where $\gamma_{\rm d}/\gamma_{\rm L} = 0.2$, and $\hat{\nu}_{\rm f} = \hat{\nu}_{\alpha} = 0$: (a) $\hat{\nu}_{\rm d} = 0.21$, (b) $\hat{\nu}_{\rm d} = 0.25$, (c) $\hat{\nu}_{\rm d} = 0.28$.

A spectrogram showing nonlinear behaviors far from marginal stability is given in Fig. 4. As mentioned above, the hole-clump pairs are formed in a dissipative system to release energy, and to balance the dissipated power. Consider the limit of small $\gamma_{\rm d}/\gamma_{\rm L} = 0.2$; here, less power is required, and thus $\delta\omega$ and its sub-branches (the minor short-lived chirping branches) are much smaller and weaker in comparison to those shown in Fig. 3(a). With an increase in the diffusion effect, which can suppress the motion of hole-clump pairs, the sub-branches gradually disappear.

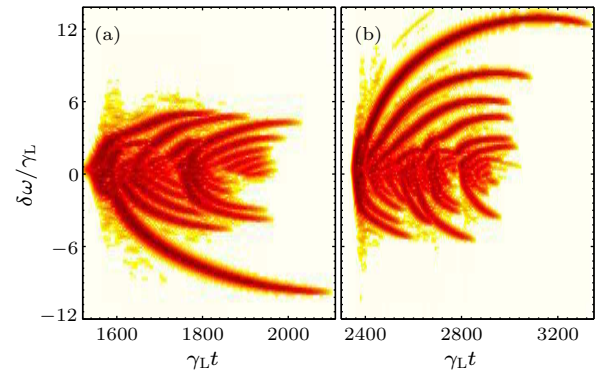

Fig. 5. Spectrogram of asymmetric frequency chirping, where $\gamma_{\rm d}/\gamma_{\rm L} = 0.9$, $\hat{\nu}_{\alpha} = 0$, and $\hat{\nu}_{\rm d} = 0.85$: (a) $\hat{\nu}_{\rm f} = 0.38$, (b) $\hat{\nu}_{\rm f} = 0.7$.

Examples of asymmetric frequency chirping in the marginal stability kinetic system with diffusion and drag are shown in Fig. 5. In cases of pure diffusion, [see Figs. 3(a) and 4] symmetric patterns are observed, and we affirm that the diffusion effect suppresses both holes and clumps. In contrast, the motion of holes is enhanced, and the clumps are suppressed, with an increase in the drag effect [Fig. 5(b)]. In general, both diffusion and drag effect can weaken the motion of clumps, and it is almost impossible to observe the downward sweeping pattern. However, we find that this phenomenon often occurs in a specific range of diffusion parameters when $\hat{\nu}_{\rm f} < \frac{1}{2}\hat{\nu}_{\rm d}$ [see Fig. 5(a)]. This is caused by a complicated interaction between diffusion and drag. In addition, Alfvén waves exhibiting downward frequency chirping are often observed in experiments.[14] Future research in this area may provide a more detailed explanation.

Another example of nonlinear behavior is mode splitting, as shown in Fig. 6. Here, we show that an original spectral line splits into a number of sidebands with equidistant and small frequency spacing. Based on the Berk–Breizman model, the mode splitting simulation results agree well with the experimental phenomena. This nonlinear dynamical evolution of the spectrum is interpreted in Ref. [24]. It occurs in marginally unstable cases with large diffusion ($\hat{\nu}_{\rm d} = 2$). The time evolution of the bounce frequency [Fig. 6(b)] indicates that it belongs to a periodic regime. Compared with frequency chirping, mode splitting has smaller disturbance amplitude, and the motion of hole-clump pairs is much weaker.

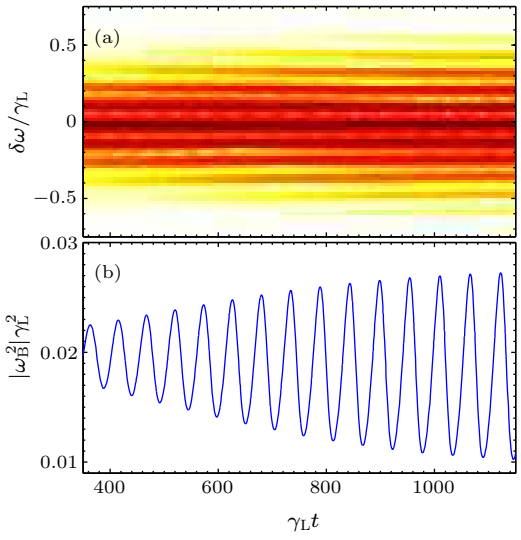

Fig. 6. (a) Spectrogram of mode splitting under conditions of marginal stability, where $\gamma_{\rm d}/\gamma_{\rm L} = 0.9$, $\hat{\nu}_{\rm d} = 2$, and $\hat{\nu}_{\rm f} = \hat{\nu}_{\alpha} = 0$. (b) Time evolution of the bounce frequency.

In summary, we have employed BOT code to simulate two typical nonlinear behaviors: frequency chirping and mode splitting. Examples of frequency chirping with and without diffusion have been presented, so as to emphasize the role of the diffusion effect in suppressing hole-clump pairs. Meanwhile, the motion

of holes is enhanced, and clumps are suppressed, with an increase in the drag effect. Downward-sweeping patterns are observed in a specific range of diffusion parameters, caused by an interaction of diffusion and drag. Discrepancies in frequency chirping between marginally and far from marginally unstable case have been presented and explained via a dissipative system. Mode splitting is produced in a marginally unstable case with large diffusion, and the motion of hole-clump pairs is much weaker. As nonlinear interactions of Alfvén waves and energetic particles are an inevitable feature of future burning fusion plasmas, nonlinear simulations of bump-on-tail instabilities are crucial for predicting and controlling the consequences of wave-particle interactions in the performance of ITER.

References

[1] Chen W and Wang Z X 2020 *Chin. Phys. Lett.* **37** 125001
[2] Wu Y B *et al.* 2019 *Chin. Phys. Lett.* **36** 045201
[3] Chen Y *et al.* 2020 *Chin. Phys. Lett.* **37** 095201
[4] Fisch N J and Herrmann M C 1994 *Nucl. Fusion* **34** 1541
[5] Heidbrink W W *et al.* 1991 *Nucl. Fusion* **31** 1635
[6] Wong K L *et al.* 1991 *Phys. Rev. Lett.* **66** 1874
[7] Wan B N and the EASteam T 2020 *Chin. Phys. Lett.* **37** 045202
[8] Chen L and Zonca F 2016 *Rev. Mod. Phys.* **88** 015008
[9] Hu W, Feng H Y and Zhang W L 2019 *Chin. Phys. Lett.* **36** 085201
[10] Heidbrink W W 1995 *Plasma Phys. Control. Fusion* **37** 937
[11] Kusama Y *et al.* 1999 *Nucl. Fusion* **39** 1837
[12] Pinches S D *et al.* 2004 *Plasma Phys. Control. Fusion* **46** S47
[13] Fredrickson E D *et al.* 2006 *Nucl. Fusion* **46** S926
[14] Hou Y M *et al.* 2018 *Nucl. Fusion* **58** 096028
[15] Lilley M K, Breizman B N and Sharapov S E 2009 *Phys. Rev. Lett.* **102** 195003
[16] Lilley M K, Breizman B N and Sharapov S E 2010 *Phys. Plasmas* **17** 092305
[17] Lilley M K and Breizman B N 2012 *Nucl. Fusion* **52** 094002
[18] Lilley M K and Nyqvist R M 2014 *Phys. Rev. Lett.* **112** 155002
[19] Lesur M *et al.* 2010 *Phys. Plasmas* **17** 122311
[20] Wang X Q *et al.* 2021 *Plasma Phys. Control. Fusion* **63** 015004
[21] Zhang H S, Lin Z and Holod I 2012 *Phys. Rev. Lett.* **109** 025001
[22] Wang X *et al.* 2012 *Phys. Rev. E* **86** 045401
[23] Zhu J, Ma Z W and Fu G Y 2014 *Nucl. Fusion* **54** 123020
[24] Fasoli A *et al.* 1998 *Phys. Rev. Lett.* **81** 5564
[25] Hole M J and Appel L C 2009 *Plasma Phys. Control. Fusion* **51** 045002
[26] Berk H L, Breizman B N and Ye H C 1992 *Phys. Rev. Lett.* **68** 3563
[27] Berk H L, Breizman B N and Pekker M 1996 *Phys. Rev. Lett.* **76** 1256
[28] Berk H L, Breizman B N and Petviashvili N V 1997 *Phys. Lett. A* **234** 213